

# Supporting Information I: Mathematical Background and Simulation Procedures for an ECEC' Mechanism at the RDE

## *Analysis of multi-electron, multi-step homogeneous catalysis by rotating disc electrode voltammetry: Theory, application, and obstacles*

Katherine J. Lee,<sup>†</sup> Cole T. Gruninger,<sup>†</sup> Kunal M. Lodaya,<sup>†</sup> Saad Qadeer,<sup>‡</sup> Boyce E. Griffith,<sup>‡</sup> and Jillian L. Dempsey<sup>†</sup>

<sup>†</sup>Department of Chemistry, University of North Carolina at Chapel Hill, Chapel Hill, North Carolina, USA 27599

<sup>‡</sup>Department of Mathematics, University of North Carolina at Chapel Hill, Chapel Hill, North Carolina, USA 27599

<i>Table of Contents</i>	<i>Page</i>
Glossary of Symbols .....	S2
SI-1 Modeling an ECEC' Mechanism at the RDE: The Hale and Nernst Diffusion Layer Approach.....	S4
Convective-diffusion equations for an ECEC' mechanism	
Derivation of the Hale Approach	
Derivation of the Nernst Diffusion Layer Approach	
SI-2 Overview of Numerical Methods.....	S11
Computational details associated with the Hale Approach	
Computational details associated with the Nernst Diffusion Layer Approach	
SI-3 Convergence of the Nernst Diffusion Layer and Hale Approach .....	S14
SI-4 Derivations of Plateau Current and FOW Analysis for an ECEC' Mechanism at the RDE.....	S17
References .....	S21

## Glossary of Symbols

### Lowercase letters:

$a$ : dimensionless substrate concentration

$b$ : dimensionless concentration of the catalytic intermediate following the second E step.

$c$ : dimensionless concentration of the catalytic intermediate following the last C step.

$i_p$ : diffusion-controlled plateau current of catalyst (A)

$i_{pl}$ : plateau current (A)

$k_{bn}$ : backward rate constant for the  $n$ th electron transfer ( $\text{cm s}^{-1}$ ),  $k_b = k_s \exp[(1 - \alpha)f(E - E^{0'})]$

$k_{fn}$ : forward rate constant for the  $n$ th electron transfer ( $\text{cm s}^{-1}$ ),  $k_f = k_s \exp[-\alpha f(E - E^{0'})]$

$k_n$ : rate constant one for the  $n$ th chemical step ( $\text{M}^{-1}\text{s}^{-1}$ )

$k_s$ : standard heterogeneous electrochemical rate constant ( $\text{cm s}^{-1}$ )

$k_{\Omega}$ : substrate-independent rate constant for the last step in the catalytic cycle ( $\text{s}^{-1}$ )

$p$ : dimensionless concentration of the catalyst.

$q$ : dimensionless concentration of the catalytic intermediate following the first E step.

$q'$ : dimensionless concentration of the catalytic intermediate following the first C step.

$r$ : radial distance from the center of the electrode (cm)

$t$ : time (s)

$x$ : distance orthogonal to the electrode surface (cm)

### Uppercase Letters:

$A$ : concentration of substrate in solution (M)

$A^*$ : bulk concentration of substrate in solution (M)

$B$ : concentration of the catalytic intermediate following the second E step (M).

$L$ : A constant characteristic of the rotation rate of the disk, and the kinematic viscosity of the solvent used,  $L = 0.51023\omega^{\frac{3}{2}}\nu^{\frac{-1}{2}}$  ( $\text{cm}^{-1}\text{s}^{-1}$ ).

$D$ : diffusion coefficient ( $\text{cm}^2/\text{s}$ )

$E$ : applied potential (V)

$E_{p/q}^0$ : standard reduction of the initial E step (V)

$E_{b/c}^0$ : standard reduction potential of the second E step (V).

$f$ :  $F/RT$  ( $V^{-1}$ )

$F$ : Faraday's constant ( $C \text{ mol}^{-1}$ )

$P$ : concentration of the starting catalyst (M).

$P^*$ : bulk concentration of starting catalyst (M).

$Q$ : concentration of the catalytic intermediate following the first E step (M).

$Q'$ : concentration of the catalytic intermediate following the first C step (M).

$R$ : gas constant ( $J \text{ mol}^{-1} \text{ K}^{-1}$ )

$S$ : surface area of the RDE ( $\text{cm}^2$ )

$T$ : temperature (K)

### Greek Letters:

$\alpha$ : transfer coefficient

$\gamma$ : the dimensionless excess factor,  $\gamma = \frac{A^*}{P^*}$

$\delta$ : thickness of diffusion layer  $\delta = 1.61D^{1/3}\nu^{1/6}\omega^{-1/2}$  (cm)

$\theta_n$ : dimensionless potential for the nth electron transfer,  $\theta = -(f)(E - E_{couple}^{0'})$

$\lambda_n$ : dimensionless rate parameter for the nth chemical step,  $\lambda = (\delta/\mu_n)^2(P^*)$

$\mu$ : thickness of reaction-diffusion layer,  $\mu = (D_{cat}/k)^{1/2}$  (cm)

$\nu$ : kinematic viscosity (cm<sup>2</sup>/s)

$\tau$ : dimensionless time parameter

$\varphi$ : Azimuthal angle measured from the center of the rotating disk (rad)

$\Psi$ : dimensionless current,  $\Psi = i/i_{pl}$

$\omega$ : Rotation rate of the rotating disk electrode (rad/s)

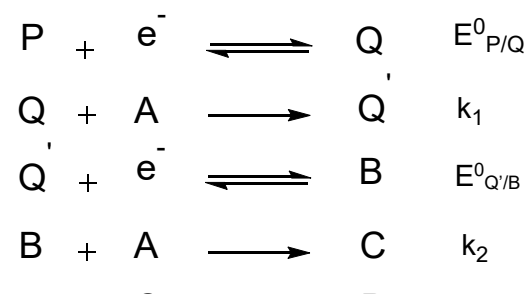
## SI-1 Modeling an ECEC' Mechanism at the RDE: The Hale and Nernst Diffusion Layer Approach

For an ECEC' process at the RDE that does not assume pseudo-first order reactivity with respect to substrate, we will need to solve, simultaneously, a system of six convective-diffusion equations with added kinetic terms. Analytical solutions to such systems do not exist; hence, numerical methods must be used to obtain approximate solutions. However, it should be noted that attempts to solve similar equations for the EC' and ECE mechanisms at steady state (setting the time derivatives to zero), using homotopic perturbation methods have been recently described.<sup>1</sup>

Two strategies were employed to simplify and solve these nonlinear reaction-convection-diffusion equations: the Hale approach and the Nernst Diffusion Layer approach. The following discussion will first describe the relevant reaction-convection-diffusion equations that must be solved and then provide the derivations for both the Hale and Nernst Diffusion Layer approaches.

### Convection-diffusion equations for an ECEC' mechanism

A general ECEC' mechanism at the RDE is given by the following set of chemical equations:



In the absence of mass transfer by migration, this system can be described by the following non-linear reaction-convection-diffusion equations:

$$\frac{\partial P}{\partial t} = D \left( \frac{\partial^2 P}{\partial x^2} \right) + Lx^2 \left( \frac{\partial P}{\partial x} \right) + k_2 BA; \quad \frac{\partial Q}{\partial t} = D \left( \frac{\partial^2 Q}{\partial x^2} \right) + Lx^2 \left( \frac{\partial Q}{\partial x} \right) - k_1 AQ;$$

$$\frac{\partial Q'}{\partial t} = D \left( \frac{\partial^2 Q'}{\partial x^2} \right) + Lx^2 \left( \frac{\partial Q'}{\partial x} \right) + k_1 AQ; \quad \frac{\partial B}{\partial t} = D \left( \frac{\partial^2 B}{\partial x^2} \right) + Lx^2 \left( \frac{\partial B}{\partial x} \right) - k_2 AB;$$

$$\frac{\partial A}{\partial t} = D \left( \frac{\partial^2 A}{\partial x^2} \right) + Lx^2 \left( \frac{\partial A}{\partial x} \right) - k_1 AQ - k_2 AB.$$

Here,  $Lx^2$  is given by a truncated series that describes the solution velocity close to the electrode surface. This is an approximate solution obtained from the Navier-Stokes equation by Von Kármán<sup>2</sup> and numerically verified by Cochran<sup>3</sup>. In this analysis, we have assumed all chemical species in solution to have identical diffusion coefficients.

One might be curious as to why these equations are posed in only one spatial dimension. The geometry and symmetry of the RDE setup make it convenient to convert the Cartesian coordinates that are commonly used when solving the mass-transfer part of an electrochemical problem to cylindrical coordinates. In cylindrical coordinates, concentrations are no longer a function of  $\varphi$  such that  $\frac{\partial C}{\partial \varphi} = 0$  (where C is a generic chemical concentration). In addition, Levich demonstrated in his seminal work *Physicochemical Hydrodynamics* that the surface of the RDE is uniformly accessible, which allows us to set  $\frac{\partial C}{\partial r} = 0$ .<sup>4</sup> Thus, we need only to focus on the coordinate orthogonal to the electrode surface, which in this case is denoted  $x$ .

To solve these partial differential equations, boundary conditions must be given for each species. Herein, Robin boundary conditions, corresponding to the use of Butler Volmer kinetics, are used. This will produce a more general solution as these boundary conditions do not assume that the Nernstian electron transfer condition holds.

The boundary conditions in the bulk solution ( $x \rightarrow \infty$ ), as well as the initial conditions ( $t = 0$ ), are then given by:

$$P(x \rightarrow \infty, t > 0) = P(x, t = 0) = P^*;$$

$$Q(x \rightarrow \infty, t > 0) = Q(x, t = 0) = 0;$$

$$Q'(x \rightarrow \infty, t > 0) = Q'(x, t = 0) = 0;$$

$$B(x \rightarrow \infty, t > 0) = B(x, t = 0) = 0;$$

$$A(x \rightarrow \infty, t > 0) = A(x, t = 0) = A^*.$$

The boundary conditions at the RDE surface ( $x = 0$ ) are given by:

$$\begin{aligned} \left(\frac{\partial P}{\partial x}\right)_{x=0} &= k_{f1}P(x=0) - k_{b1}Q(x=0); & \left(\frac{\partial Q'}{\partial x}\right)_{x=0} &= k_{f2}Q'(x=0) - k_{b2}B(x=0); \\ \left(\frac{\partial Q}{\partial x}\right)_{x=0} &= -\left(\frac{\partial P}{\partial x}\right)_{x=0}; & \left(\frac{\partial Q'}{\partial x}\right)_{x=0} &= -\left(\frac{\partial B}{\partial x}\right)_{x=0}; \\ & & \left(\frac{\partial A}{\partial x}\right)_{x=0} &= 0; \end{aligned}$$

where the forward and backward electron transfer rate constants are defined in terms of the standard Butler Volmer kinetics treatment.<sup>5</sup>

### Derivation of the Hale Approach

Now that we have the appropriate initial and boundary conditions, we begin with our derivation of the Hale approach. First, the system of equations are cast into dimensionless forms by introducing the following set of variables:

$$\begin{aligned} W &= \left(\frac{L}{D}\right)^{\frac{1}{3}}x; & \tau &= (L^2D)^{\frac{1}{3}}t; & \lambda_1 &= k_1P^*L^{-\frac{2}{3}}D^{-\frac{1}{3}}; & \lambda_2 &= k_2P^*L^{-\frac{2}{3}}D^{-\frac{1}{3}}; \\ \gamma &= \frac{A^*}{P^*}; & a &= \frac{A}{P^*}; & p &= \frac{P}{P^*}; & q &= \frac{Q}{P^*}; & q' &= \frac{Q'}{P^*}; & b &= \frac{B}{P^*}. \end{aligned}$$

After re-writing the equations in dimensionless forms, application of the chain rule to the aforementioned convective diffusion equations yields:

$$\begin{aligned} \frac{\partial p}{\partial \tau} &= \left(\frac{\partial^2 p}{\partial W^2}\right) + W^2 \left(\frac{\partial p}{\partial x}\right) + \lambda_2 ba; & \frac{\partial q}{\partial \tau} &= \left(\frac{\partial^2 q}{\partial W^2}\right) + W^2 \left(\frac{\partial q}{\partial x}\right) - \lambda_1 aq; \\ \frac{\partial q'}{\partial \tau} &= \left(\frac{\partial^2 q'}{\partial W^2}\right) + W^2 \left(\frac{\partial q'}{\partial x}\right) + \lambda_1 aq; & \frac{\partial b}{\partial \tau} &= \left(\frac{\partial^2 b}{\partial W^2}\right) + W^2 \left(\frac{\partial b}{\partial x}\right) - \lambda_2 ab; \\ \frac{\partial a}{\partial \tau} &= \left(\frac{\partial^2 a}{\partial W^2}\right) + W^2 \left(\frac{\partial a}{\partial x}\right) - \lambda_2 ab - \lambda_1 aq. \end{aligned}$$

The Hale transformation<sup>6</sup> then provides another coordinate transformation given by the following equation, where  $\int_0^\infty e^{-W'^3/3} dW' = \sqrt{1.65894}$ :

$$Y = \frac{\int_0^W e^{-W'^3/3} dW'}{\int_0^\infty e^{-W'^3/3} dW'}.$$

The Hale transformation in effect reduces the two terms corresponding to diffusion and convection into a single expression. This transforms what was a semi-infinite domain, to a finite domain where  $x = 0$  corresponds to  $Y = 0$ , and  $x = \infty$  corresponds to  $Y = 1$ .

Following the use of the Hale transformation, the system of equations is boiled down to:

$$\begin{aligned}\frac{\partial p}{\partial \tau} &= \frac{e^{-\frac{2W^3}{3}}}{1.65894} \left( \frac{\partial^2 p}{\partial Y^2} \right) + \lambda_2 ba; & \frac{\partial q}{\partial \tau} &= \frac{e^{-\frac{2W^3}{3}}}{1.65894} \left( \frac{\partial^2 q}{\partial Y^2} \right) - \lambda_1 aq; \\ \frac{\partial q'}{\partial \tau} &= \frac{e^{-\frac{2W^3}{3}}}{1.65894} \left( \frac{\partial^2 q'}{\partial Y^2} \right) + \lambda_1 aq; & \frac{\partial b}{\partial \tau} &= \frac{e^{-\frac{2W^3}{3}}}{1.65894} \left( \frac{\partial^2 b}{\partial Y^2} \right) - \lambda_2 ba; \\ & & \frac{\partial a}{\partial \tau} &= \frac{e^{-\frac{2W^3}{3}}}{1.65894} \left( \frac{\partial^2 a}{\partial Y^2} \right) - \lambda_2 ab - \lambda_1 aq.\end{aligned}$$

The  $W$  coordinate can be related to the  $Y$  coordinate via:

$$\frac{dW}{dY} = \sqrt{1.65894} \exp\left(-\frac{W^3}{3}\right).$$

This equation is solved in our simulation program with a standard fourth order Runge-Kutta method.

In addition, new values corresponding to the initial conditions ( $\tau = 0$ ) and boundary conditions in the bulk solution ( $Y = 1$ ) are given by:

$$p(Y = 1, \tau > 0) = p(Y, \tau = 0) = 1; \quad q(Y = 1, \tau > 0) = q(Y, \tau = 0) = 0;$$

$$q'(Y = 1, \tau > 0) = q'(Y, \tau = 0) = 0; \quad b(Y = 1, \tau > 0) = b(Y, \tau = 0) = 0;$$

$$a(Y = 1, \tau > 0) = a(Y, \tau = 0) = \gamma.$$

And the boundary conditions at the surface of the RDE ( $Y = 0$ ) become

$$\left( \frac{\partial p}{\partial Y} \right)_{Y=0} = K_{f_1} p(Y = 0) - K_{b_1} q(Y = 0);$$

$$\left( \frac{\partial b}{\partial Y} \right)_{Y=0} = K_{f_2} b(Y = 0) - K_{b_2} c(Y = 0);$$

$$\left( \frac{\partial q}{\partial Y} \right)_{Y=0} = - \left( \frac{\partial p}{\partial Y} \right)_{Y=0}; \quad \left( \frac{\partial b}{\partial Y} \right)_{Y=0} = - \left( \frac{\partial q'}{\partial Y} \right)_{Y=0};$$

$$\left(\frac{\partial a}{\partial Y}\right)_{Y=0} = 0;$$

where  $K_{f/b} = \sqrt{1.65894}k_{f/b}(L^2D)^{1/3}$ .

If we define cathodic current as positive, the dimensionless current is given by

$$\Psi = \frac{\sqrt{1.65894}i}{nFSP^*(D^2L)^{1/3}} = \left(\left(\frac{\partial p}{\partial Y}\right)_{Y=0} + \left(\frac{\partial b}{\partial Y}\right)_{Y=0}\right).$$

With these simplified equations and coordinate space, discretization via finite differences can be employed to determine the current potential curves of interest.

### **Derivation of the Nernst Diffusion Layer Approach**

The Nernst Diffusion Layer approach simplifies the reaction-convection-diffusion equation tremendously by stipulating the existence of a layer at the electrode surface with a thickness  $\delta$  in which convective effects can be neglected. In this model, for any  $x < \delta$ , the convection term within the given system of differential equations can be eliminated. The thickness of this diffusion layer is given by:

$$\delta = 1.61D^{1/3}\nu^{1/6}\omega^{-1/2}.$$

The thickness of the diffusion layer can be experimentally modulated via rotation rate, whereby faster rotation rates result in thinner diffusion layers.



As RDE rapidly achieves steady state conditions (at slow scan rates), we must now solve the steady-state version of Fick's second law for  $0 \leq x \leq \delta$ . Hence, we will apply the use of finite boundary conditions stipulated at both the electrode surface and at the edge of the Nernst diffusion layer. The equations to solve for the ECEC' reaction mechanism are then given by:

$$D \left( \frac{d^2 P}{dx^2} \right) = -k_2 B A; \quad D \left( \frac{d^2 Q}{dx^2} \right) = k_1 A Q; \quad D \left( \frac{d^2 Q'}{dx^2} \right) = -k_1 Q A; \quad D \left( \frac{d^2 B}{dx^2} \right) = k_2 B A;$$

$$D \left( \frac{d^2 A}{dx^2} \right) = k_1 Q A + k_2 B A.$$

The boundary conditions at the diffusion layer ( $x = \delta$ ) are given by:

$$P(x = \delta) = P^*; \quad Q(x = \delta) = 0;$$

$$Q'(x = \delta) = 0; \quad B(x = \delta) = 0;$$

$$A(x = \delta) = A^*.$$

At the electrode surface ( $x = 0$ ), we now use the Nernstian electron transfer boundary conditions to obtain

$$\frac{(P)_{x=0}}{(Q)_{x=0}} = \exp\left(\frac{F}{RT}(E - E_{P/Q}^0)\right); \quad \frac{(Q')_{x=0}}{(B)_{x=0}} = \exp\left(\frac{F}{RT}(E - E_{Q'/B}^0)\right);$$

$$\left(\frac{dP}{dx}\right)_{x=0} = -\left(\frac{dQ}{dx}\right)_{x=0}; \quad \left(\frac{dB}{dx}\right)_{x=0} = -\left(\frac{dQ'}{dx}\right)_{x=0};$$

$$\left(\frac{dA}{dx}\right)_{x=0} = 0.$$

We then introduce the following dimensionless parameters:

$$y = \frac{x}{\delta}; \quad \lambda_1 = \frac{k_1 \delta^2 P^*}{D}; \quad \lambda_2 = \frac{k_2 \delta^2 P^*}{D}; \quad \gamma = \frac{A^*}{P^*};$$

$$p = \frac{P}{P^*}; \quad q = \frac{Q}{P^*}; \quad q' = \frac{Q'}{P^*}; \quad b = \frac{B}{P^*}; \quad a = \frac{A}{P^*}.$$

Substituting these dimensionless variables into our differential equation yields the following set of dimensionless differential equations

$$\left(\frac{d^2p}{dy^2}\right) = -\lambda_2ba; \quad \left(\frac{d^2q}{dy^2}\right) = \lambda_1aq; \quad \left(\frac{d^2q'}{dy^2}\right) = -\lambda_1aq; \quad \left(\frac{d^2b}{dy^2}\right) = \lambda_2ab;$$

$$\left(\frac{d^2a}{dy^2}\right) = \lambda_1aq + \lambda_2ab.$$

Substitution of the dimensionless variables into the  $y = 1$  boundary condition gives

$$p(y = 1) = 1; \quad q(y = 1) = 0;$$

$$q'(y = 1) = 0; \quad b(y = 1) = 0;$$

$$a(y = 1) = \gamma.$$

Substitution of dimensionless variables for the boundary conditions at the surface of the electrode ( $y = 0$ ) yields

$$\frac{(p)_{y=0}}{(a)_{y=0}} = \exp(\theta); \quad \frac{(q')_{y=0}}{(b)_{y=0}} = \exp(\theta');$$

$$\left(\frac{dp}{dy}\right)_{y=0} = -\left(\frac{dq}{dy}\right)_{y=0}; \quad \left(\frac{db}{dy}\right)_{y=0} = -\left(\frac{dq'}{dy}\right)_{y=0};$$

$$\left(\frac{da}{dy}\right)_{y=0} = 0;$$

where  $\theta$  and  $\theta'$  represent the dimensionless potential terms defined as

$$\theta = \frac{F}{RT} \left( E - E_{P/Q}^0 \right); \quad \theta' = \frac{F}{RT} \left( E - E_{Q'/B}^0 \right).$$

Again taking cathodic current to be positive, the dimensionless current  $\Psi$  is determined by

$$\Psi = \frac{\delta i}{\text{FSDP}^*} = \left(\frac{dp}{dy}\right)_{y=0} + \left(\frac{db}{dy}\right)_{y=0}.$$

These equations can be readily approximated via standard numerical methods.

## SI-2 Overview of Numerical Methods

### Computational Details Associated with the Hale Approach

Equations derived via the Hale transform were numerically solved in time using the backward Euler method, which is an implicit method. We use an implicit method to avoid numerical instabilities related to the nonlinear kinetic terms that appear for explicit time stepping schemes. The stiffness typically associated with the diffusion terms motivated the use of a fully implicit method.

To describe our computational approach, the unit interval, corresponding to the computational domain and the entire physical domain by application of the Hale transformation, is split up into  $N$  intervals of equal length using a total of  $N+1$  grid points. The second derivatives are approximated by a standard three-point second-order centered finite difference formula. For the duration of the simulation, a time step size of  $5e-3$  was maintained for each time step, and the resulting nonlinear system was solved using the Newton-Raphson method with an error tolerance fixed at  $1e-8$ . Since we are interested in solving for the current-potential response under steady-state conditions – as is realized experimentally with RDE – the following approach is used: For the initial time point ( $t = 0$ ), the potential is held at a value sufficiently positive of the reduction potential of the catalyst such that no current flows. The potential is then stepped to a value where current begins to flow and the transient current response is computed until deviation from steady-state is negligible. This process is then repeated iteratively until the potential reaches its pre-determined switching potential. The current-potential response for a simple, reversible one-electron reduction was calculated in order to test the validity of this numerical approach. The mass transport corrected Tafel plot of  $\theta$  against  $\log_{10}(i^{-1} - i_{pl}^{-1})$  for the resulting waveform were found to have the required slope of  $2.303^7$  (Figure S1), validating this numerical approach.

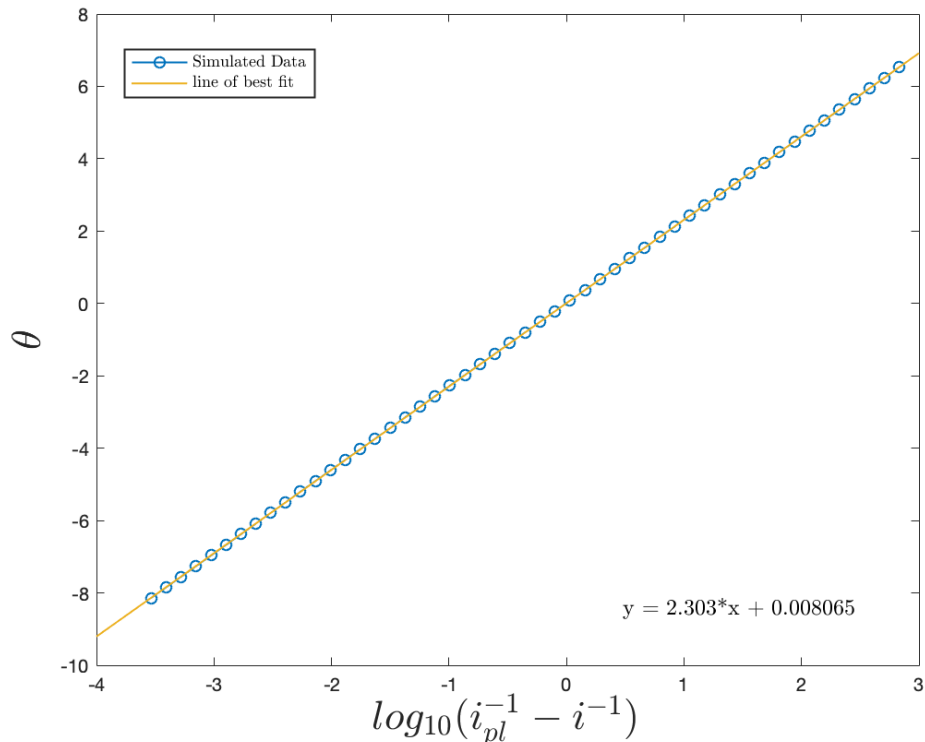


**Figure S1:** Mass transport corrected Tafel analysis of current-potential curves for a single reversible electron transfer. As the line of best fit shows, the required slope of 2.303 was achieved.

### Computational Details Associated with the Nernst Diffusion Layer Approach

The equations obtained from the Nernst Diffusion Layer approach were also approximated by a finite difference formula with the Newton-Raphson method used for solving the resulting nonlinear equations. To more accurately resolve the dynamics close to the electrode surface, we employed a nonuniform grid in this regime paired with a Newton-Raphson error tolerance set to  $1e-10$ . More specifically, the domain  $[0, \delta]$  was split into  $N$  intervals with grid-points  $x_i = i^2 h$ , for  $i = 0, 1, 2, \dots, N$  where  $h = \frac{\delta}{N^2}$ . This requires non-uniform finite differences formulas.<sup>8</sup> Steady-state current-potential curves and concentration profiles were computed in an iterative manner by first holding the potential sufficiently positive such that no current is passed. From this point, the potential is then stepped and the current-potential behavior and concentration profiles are computed. This process is then repeated over the entire potential window. Again, the validity of this approach was verified by calculating the response for a single, reversible electron transfer

reaction and performing mass transport corrected Tafel analysis on the resulting trace. The required slope of 2.303 was also achieved for this numerical approach (Figure S2).

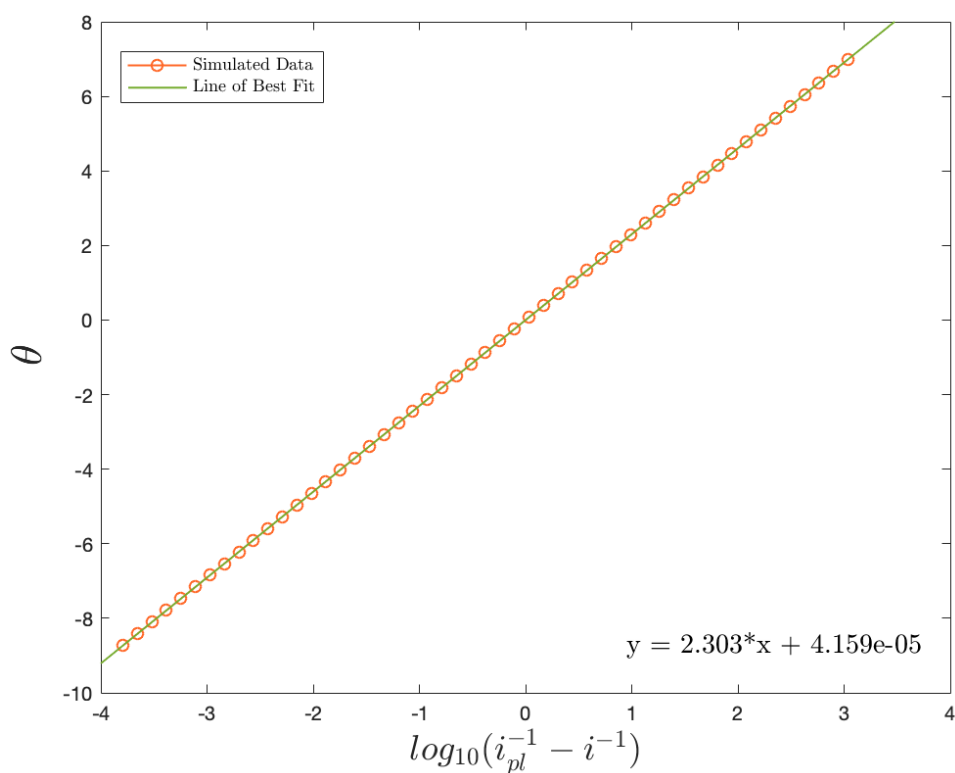


**Figure S2:** Mass transport corrected Tafel analysis for single reversible electron transfer current-potential curves using the Nernst Diffusion Layer approximation method. As the line of best fit shows, the required slope of 2.303 was obtained.

Finally, we remark that both the Nernst Diffusion Layer and Hale Transformation numerical models were originally designed to incorporate a final chemical step corresponding to the ECECC' mechanism of the cobaloxime catalyst.<sup>9</sup> This third chemical step is included in the MATLAB scripts. In order to negate any effects of this last chemical step on the ECEC' current-potential curves of interest described here and in the main text, the homogenous rate constant,  $k_3$ , was set to equal to a  $\log_{10}$  value of 15 for each simulated voltammograms. However, any of the rate constants within the simulation script can easily be toggled to also incorporate different reaction mechanisms such as EC, ECE, ECEC, ECEC', and ECECC' so long as the homogenous and heterogenous rate constants are chosen accordingly.

### SI-3 Convergence of the Nernst Diffusion Layer and Hale Approach

The dimensionless rate parameter associated with both numerical methods can be identified by rewriting the parameter  $\delta$  (describing the diffusion layer thickness) in terms of  $L$  using the following equation:

$$\delta = 1.288 \left( \frac{D}{L} \right)^{1/3}.$$

Identifying these dimensionless parameters facilitates comparison of the two numerical methods over a wide range of rate constants, rotation rates, and acid concentrations.

By confirming agreement between the two methods under the *pure kinetic conditions* of interest, we may solve for rate constants using plateau current and FOW analysis as derived in the next section. In addition to the plots shown in the main text, we have provided two others (Figure S3 and Figure S4) which further demonstrate the agreement of both methods under *pure kinetic conditions*. To restate, this agreement between both the Nernst Diffusion Layer and Hale Transformation models allows us to simplify what was a second order partial differential equation with respect to time and space (the convective diffusion equations on page S6), to a second order ordinary, constant coefficient, differential equation (page introduction to the Nernst Diffusion Layer Approach on page S9) that can be easily solved for the homogenous rate constants  $k_1$  and  $k_2$  via plateau current analysis and foot-of-the-wave analysis when *pure kinetic conditions* hold (see SI-4).

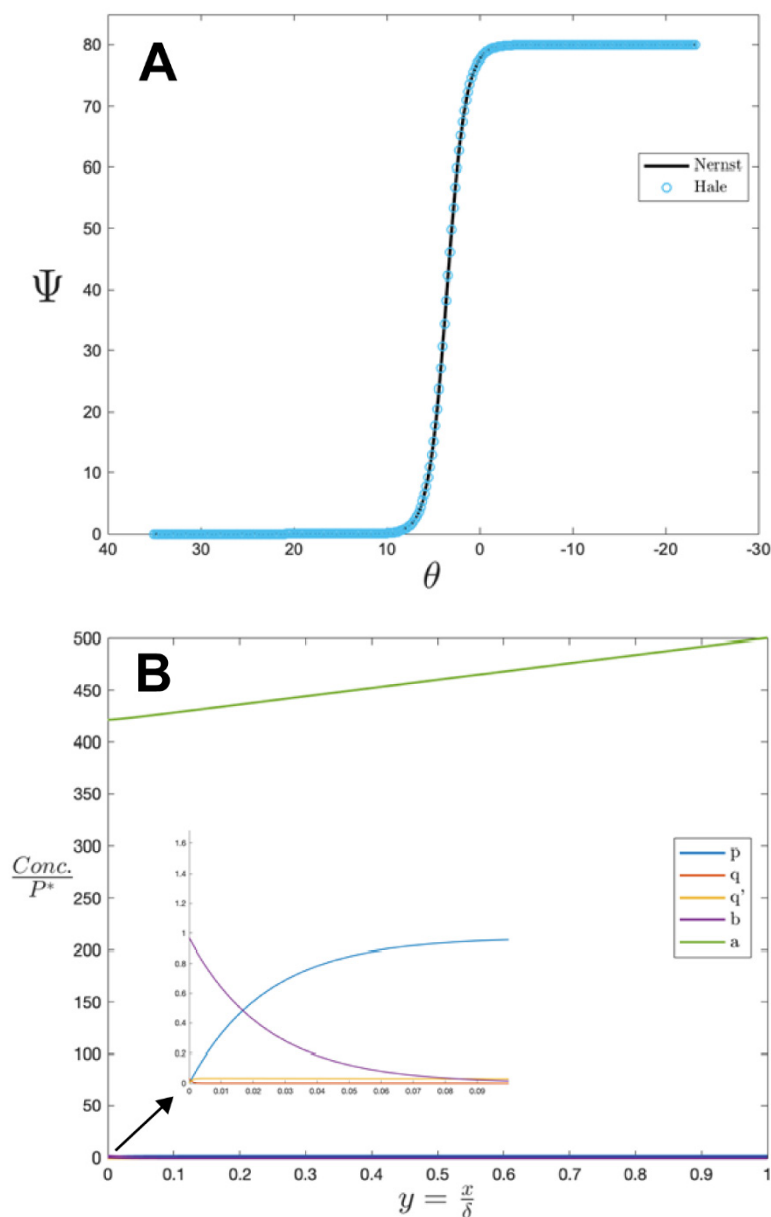


**Figure S3: (A)** Simulated catalytic ECEC' RDE waveforms comparing both the Nernst Diffusion Layer and Hale Transformation approaches under *pure kinetic conditions*. Here, reversible electron transfer was assumed,  $\gamma$  was set to value of 500, and homogenous rate constants were fixed such that  $k_1 = 1 \times 10^7 M^{-1} s^{-1}$  and  $k_2 = 1 \times 10^5 M^{-1} s^{-1}$ . Both the Nernst Diffusion Layer and Hale Transformation approaches show great agreement in this regime. **(B)** Corresponding simulated dimensionless concentration profiles. Here  $p, q, q', b,$  and  $a$  hold the same definitions as they did in SI-2. As one can see, the consumption of  $a$  is negligible with respect to the concentration of the catalytic intermediates which are contained to a thin reaction-diffusion layer much smaller than the Nernst diffusion layer itself.

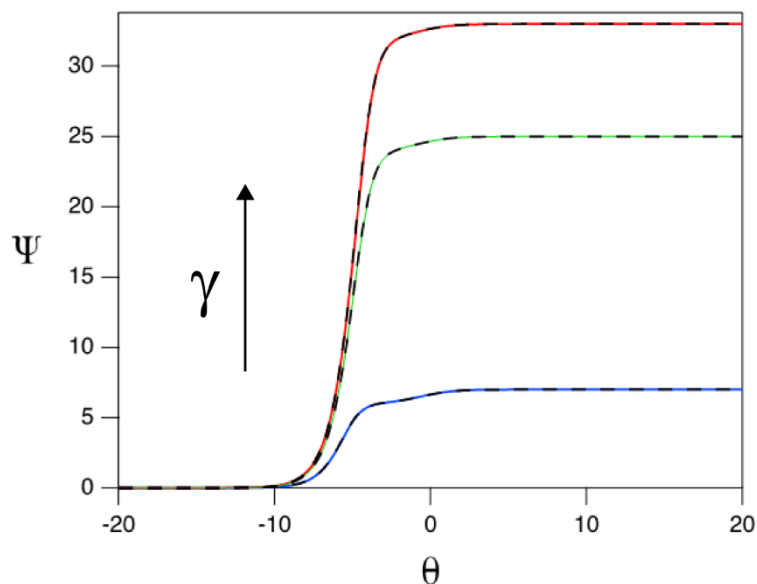


**Figure S4** Simulated RDE voltammograms for an ECEC' catalytic mechanism utilizing the Hale transformation approach (dotted lines) and the Nernst Diffusion Layer approximation approach (solid lines). Here, dimensionless rate parameters for both models were equated and set to a log value of 5.  $\gamma$  values were then sampled at values of 6 (dark blue), 24 (green), and 32 (red). As  $\gamma$  is increased, the splitting feature of the pre-catalytic waveform becomes masked and eventually disappears altogether corresponding to transition between total-catalysis and mixed-transport kinetic control.



## SI-4 Derivations of Plateau Current and Foot-of-the-Wave Analysis for an ECEC' Mechanism at the RDE

In order to begin the derivations for plateau current and foot-of-the-wave, we first must obtain a mathematical expression for the current-potential response under pure kinetic conditions in the absence of substrate consumption. Analogous derivations have been done for a myriad of two-electron, two-step catalytic reaction schemes using features pertinent to stationary electrochemistry.<sup>2</sup> The subsequent analysis differs from that of stationary methods in that all time derivatives are set to zero (as RDE involves steady-state mass transport) and finite boundary conditions are stipulated rather than semi-infinite ones. As expected, despite these differences in approach, the same mathematical expression is derived for the steady-state catalytic response in both cases. We start with equations of the ECEC' mechanism and the boundary conditions invoked in the introduction of the Nernst Diffusion Layer Approach (page S9):

$$D \left( \frac{d^2 P}{dx^2} \right) = -k_2 BA; \quad D \left( \frac{d^2 Q}{dx^2} \right) = k_1 AQ; \quad D \left( \frac{d^2 Q'}{dx^2} \right) = -k_1 QA;$$

$$D \left( \frac{d^2 B}{dx^2} \right) = k_2 BA; \quad D \left( \frac{d^2 A}{dx^2} \right) = k_1 QA + k_2 BA.$$

Additionally, Fick's first law is included in this analysis, as given by

$$\left( \frac{dP}{dx} \right)_{x=0} = - \left( \frac{dQ}{dx} \right)_{x=0} = \frac{i_1}{FSD};$$

$$\left( \frac{dQ'}{dx} \right)_{x=0} = - \left( \frac{dB}{dx} \right)_{x=0} = \frac{i_2}{FSD};$$

where  $i_1 + i_2 = i$ .

Now, using the linearity of the differential operator, we can combine each catalytic term to produce

$$D \left( \frac{d^2(P+Q+Q'+B)}{dx^2} \right) = 0,$$

which upon integration and application of the relevant boundary conditions yields

$$P + Q + Q' + B = P^*.$$

Moreover, we solved the equation above for all  $0 \leq x \leq \delta$ , we have that at  $x = 0$

$$(P)_{x=0} + (Q)_{x=0} + (Q')_{x=0} + (B)_{x=0} = P^*.$$

And if we recall the Nernstian electron transfer boundary conditions, we can show that

$$(Q)_{x=0}(1 + \exp(\theta_1)) + (B)_{x=0}(1 + \exp(\theta_2)) = P^*.$$

Now with this equation in mind, and recalling that because of our assumption that the substrate concentration is in essence fixed at the electrode surface, we now go back to our original differential equations to solve for both  $(Q)_{x=0}$  and  $(B)_{x=0}$ :

$$D \left( \frac{d^2 Q}{dx^2} \right) = k_1 A Q;$$

$$D \left( \frac{d^2 B}{dx^2} \right) = k_2 B A.$$

Solving both linear, constant coefficient, second order differential equations with the application of the relevant boundary conditions and the use of Fick's first law then yields

$$Q(x) = \frac{i_1 \exp\left(-\sqrt{\frac{k_1 A}{D}} x\right)}{FS\sqrt{D}\sqrt{k_1 A}(1 + \exp(-2\delta\sqrt{\frac{A k_1}{D}}))} - \frac{i_1 \exp\left(\sqrt{\frac{k_1 A}{D}}(x - 2\delta)\right)}{FS\sqrt{D}\sqrt{k_1 A}(1 + \exp\left(-2\delta\sqrt{\frac{k_1 A}{D}}\right))};$$

$$B(x) = \frac{i_2 \exp\left(-\sqrt{\frac{k_2 A}{D}} x\right)}{FS\sqrt{D}\sqrt{k_2 A}(1 + \exp(-2\delta\sqrt{\frac{k_2 A}{D}}))} - \frac{i_2 \exp\left(\sqrt{\frac{k_2 A}{D}}(x - 2\delta)\right)}{FS\sqrt{D}\sqrt{k_2 A}(1 + \exp\left(-2\delta\sqrt{\frac{k_2 A}{D}}\right))}.$$

However, because of our assumption of *pure kinetic conditions*,  $k_1 A$  and  $k_2 A$  are very large in magnitude, and hence, the  $\exp(-2\delta\sqrt{\frac{k_{1,2} A}{D}})$  terms are well approximated by zero. With this simplification, we find that at the electrode surface ( $x = 0$ ), the equations for  $Q$  and  $B$  simplify to

$$(Q)_{x=0} = \frac{i_1}{FS\sqrt{D}\sqrt{k_1 A}};$$

$$(B)_{x=0} = \frac{i_2}{FS\sqrt{D}\sqrt{k_2 A}}.$$

Using these equations with the Nernst relation, we obtain

$$\frac{i_1}{FS\sqrt{D}\sqrt{k_1A}}(1 + \exp(\theta)) + \frac{i_2}{FS\sqrt{D}\sqrt{k_2A}}(1 + \exp(\theta')) = P^*.$$

Furthermore, under *pure kinetic conditions* we obtain that  $i_1 = i_2 = \frac{i}{2}$  thus allowing us to write

$$\frac{i}{2FS\sqrt{D}\sqrt{k_1A}}(1 + \exp(\theta)) + \frac{i}{2FS\sqrt{D}\sqrt{k_2A}}(1 + \exp(\theta')) = P^*.$$

It is here that we now set the  $\exp(\theta')$  term to zero. This simplification stems from the assumption that for our ECEC' reaction mechanism, the second electron transfer is far more thermodynamically favorable than the first. Thus, by the time any  $Q'$  forms at the electrode surface,  $\theta_2$  is negative and thus the  $\exp(\theta')$  term quickly approaches zero. This allows us to write

$$\frac{i}{2FS\sqrt{D}\sqrt{k_1A}}(1 + \exp(\theta)) + \frac{i}{2FS\sqrt{D}\sqrt{k_2A}} = P^*.$$

Solving for  $i$  now gives that

$$i = \frac{2FS\sqrt{D}\sqrt{A}P^*}{\frac{1+\exp(\theta)}{\sqrt{k_1}} + \frac{1}{\sqrt{k_2}}}.$$

And at the plateau, where  $\theta_1 \ll 0$ , we obtain the equation for  $i_{pl}$  given by

$$i_{pl} = \frac{2FS\sqrt{D}\sqrt{A}P^*}{\frac{1}{\sqrt{k_1}} + \frac{1}{\sqrt{k_2}}}.$$

And in addition, if  $k_2 \ll k_1$ , the equation can be further simplified to

$$i_{pl} = 2FS\sqrt{D}\sqrt{A^*k_2}P^*.$$

This is identical to Equation 2 in the main text, where here  $n=2$ , the geometric electrode surface area  $A$  is written as  $S$ ,  $C_P^0 = P^*$ , and  $k_{obs} = k_2 A^*$ .

Now that we have the equation for the plateau current, let's go back to the equation

$$i = \frac{2FS\sqrt{D}\sqrt{A}P^*}{\frac{1 + \exp(\theta)}{\sqrt{k_1}} + \frac{1}{\sqrt{k_2}}}$$

From this relation, we can see that at the foot of the catalytic wave, when  $\theta \gg 0$  (i.e.  $E \gg E_{P/Q}$ ), the exponential term dominates the denominator, and thus the equation for the current at the foot of the catalytic RDE wave is

$$i_{FOWA} = \frac{2FS\sqrt{D}\sqrt{k_1}AP^*}{1 + \exp(\theta)}$$

This is identical to Equation 2 in the main text, where here  $n=2$ , the geometric electrode surface area  $A$  is written as  $S$ ,  $C_P^0 = P^*$ , and  $k_{FOWA} = k_1 A$ .

## References

- (1) Saravanakumar, R.; Pirabaharan, P.; Rajendran, L. The Theory of Steady State Current for Chronoamperometric and Cyclic Voltammetry on Rotating Disk Electrodes for EC' and ECE Reactions. *Electrochim. Acta* **2019**, *313*, 441–456.
- (2) Rountree, E. S.; Martin, D. J.; McCarthy, B. D.; Dempsey, J. L. Linear Free Energy Relationships in the Hydrogen Evolution Reaction: Kinetic Analysis of a Cobaloxime Catalyst. *ACS Catal.* **2016**, *6*, 3326–3335.
- (3) Kármán, T. V. Über Laminare Und Turbulente Reibung. *ZAMM - J. Appl. Math. Mech. / Zeitschrift für Angew. Math. und Mech.* **1921**, *1* (4), 233–252.
- (4) Cochran, W. G. The Flow Due to a Rotating Disc. *Math. Proc. Cambridge Philos. Soc.* **1934**, *30*, 365–375.
- (5) Levich, V. G. *Physicochemical Hydrodynamics*; Prentice-Hall: Englewood Cliffs, NJ, USA, 1962.
- (6) Bard, A. J.; Faulkner, L. R. *Electrochemical Methods: Fundamentals and Applications*, 2nd ed.; Harris, D., Swain, E., Robey, C., Aiello, E., Eds.; John Wiley & Sons, Inc.: Hoboken, NJ, USA, 2001.
- (7) Albery, W. J. *Electrode Kinetics*; Clarendon Press, 1975.
- (8) Sundqvist, H.; Veronis, G. A Simple Finite-Difference Grid with Non-Constant Intervals. *Tellus* **1970**, *22*, 26–31.